

## Synthesis and Characterization of Silver Nanoparticles in a Nanoporous Glass

V. G. Arakcheev<sup>a</sup>, A. N. Bekin<sup>a</sup>, Yu. V. Vladimirova<sup>a</sup>, N. V. Minaev<sup>b</sup>,  
V. B. Morozov<sup>a</sup>, and A. O. Rybaltovskii<sup>c</sup>

<sup>a</sup> Department of Physics and International Laser Center, Moscow State University, Moscow, 119991 Russia

<sup>b</sup> Institute of Laser and Information Technology, Russian Academy of Sciences, Troitsk, Moscow Region, 142190 Russia

<sup>c</sup> Skobel'tsyn Institute of Nuclear Physics, Moscow State University, Moscow, 119991 Russia

e-mail: arakcheev@physics.msu.ru

Received February 17, 2014; in final form, March 8, 2014

**Abstract**—We obtained a metal-dielectric composite by thermal restoration of silver atoms from an alcohol solution of a precursor in nanoporous glass with pores with a radius of 2 nm. The concentration, size, and asphericity degree of metal nanoparticles formed in the pores are characterized according to the measured extinction spectra of the material.

**Keywords:** metal-dielectric composite, nanoparticles, nanopores, nanoporous glass, nanoplasmonics, extinction, spectroscopy.

**DOI:** 10.3103/S0027134914030035

### INTRODUCTION

Metal nanoparticles have unique properties, which makes it possible to use them in a wide range of applications related to catalysis, medical diagnostics, and therapy to design advanced optical materials with extraordinary properties. It is an urgent problem to develop the methods of creating and diagnostics of functional materials and systems that contain metal particles. Recently, the technology of planar structures formed on a flat surface is the most rapidly developing one. The growing interest in such systems is due to the high accuracy of manufacturing and ease of diagnostics. Modern technologies allow one to obtain not only the films with a desired morphology and thickness, but also separately located nanoparticles and their ensembles with well-controlled shapes, sizes and topologies. Using electron-microscopy methods one can successfully perform diagnostics of these systems when obtaining the images of particles with sizes up to a few nanometers.

An equally attractive option is the fabrication of bulk functional materials with nanosized metallic inclusions. One of the methods in the implementation of this idea is the introduction of metal nanoparticles inside nanoporous materials. In recent years successful works have demonstrated the ability to introduce the nanoparticles directly into the pores, as well as to form these particles inside the pores [1–3]. This method is especially important for nanopores of small diameter, when the penetration of fabricated nanoparticles is difficult or impossible. By themselves, nanoporous materials have many promising technological

applications involving cleaning, catalysis, adsorption, separate storage, and transportation of active substances [4, 5]. Nanoscale metallic inclusions make it possible to modify the physical and chemical properties of a material to optimize and create entirely new possibilities for applications. The diagnostics of such bulk composites involves a number of features. The use of electron microscopy in this case requires the fabrication of samples which are suitable for diagnostics, which is often difficult. First, the characteristics of the initial material should not vary in the process of manufacturing the sample. Second, to describe the statistical properties of an ensemble of nanoparticles, it is necessary to obtain a sufficiently large number of images. Due to this, the use of electron microscopy is often time-consuming and expensive.

Currently, extinction spectroscopy is increasingly used for the diagnostics of bulk composite materials and media. This method allows one to characterize the entire ensemble of nanoparticles when performing a single measurement. Resonance properties of nanoparticles cause the appearance of sharp peaks in the extinction spectrum corresponding to their plasmonic modes. The shape and position of the peaks depend on the shapes and sizes of nanoparticles, as well as on the material of the particles and surrounding dielectric medium. Comparison with the results obtained by other methods, including the use of electron microscopy shows good agreement [6–11], although some differences exist [12].

In this paper we consider the fabrication and diagnostics of a composite nanoporous glass (Vycor) [13],

in the pores of which silver particles are arranged. This type of glass has a developed grid of quasicylindrical interconnected pores with a diameter of few nanometers. To create the composite, a methodology was used that is based on the formation of nanoparticles directly within the pores [14–16]. The modeling was carried out using the extinction spectra of the sample. This allowed us to make conclusions on the concentrations, sizes, and shapes of nanoparticles. A comparison with a similar composite obtained previously using the same methods was carried out in [15, 16].

### 1. A Technique for the Formation and Diagnostics of Nanoparticles in the Pores of a Matrix

The pore radius in Vycor is  $\sim 2$  nm. The procedure of fabrication of the composite is based on the clustering of metal atoms recovered from a solution of a silver-containing precursor, which fills the pores. This approach allows one to form nanoparticles in the pores with a characteristic size of several tens of nanometers. Its effectiveness is confirmed by successful fabrication of composites with nanoparticles of different sizes, based on the matrices of various porous materials, such as glass, opals, and polymer structures [15, 16]. The specimen was impregnated with a solution of an Ag(hfac)COD precursor (Aldrich Chemical Comp. USA) in ethanol with a precursor concentration of about 10 mg/l. The sample was then annealed at a temperature of 70°C for about 20 minutes. The annealing process was accompanied by the appearance of a yellow hue, which became more saturated with time. Previously, to create a similar composite, supercritical carbon dioxide [15, 16] was used and specialized equipment was needed to maintain supercritical conditions. The use of ethanol for the impregnation allows one to perform the fabrication of a composite under ordinary conditions without any specific devices.

Diagnostics of the nanoparticle formation was carried out when recording the extinction spectra using a Specord M40 double-beam spectrograph (Carl Zeiss, Germany). Annealing of the sample was accompanied by the appearance of a pronounced peak due to absorption at the frequency of plasmon resonance of the particles. Measurement of the spectra was carried out again a few days after annealing and did not reveal significant changes, which confirms the stability of the composite.

### 2. A Model Description of the Extinction Spectra

In this paper, the characteristics of nanoparticles were determined by modeling the observed extinction spectrum. A detailed description of the model of nanoparticles as plasmonic structures can be found, for example, in [17]. The totality of the results in many studies indicates that this consideration is adequate up to the sizes of  $\sim 2$  nm. With further reduction of the

size of nanoparticles and the number of atoms, an important role is played by the size-quantization effects. The first description of these effects was probably presented in [18]. The exact threshold for the transition from plasmonic to quantum mode depends on the type of metal and homogeneity of its structure, which is determined by the conditions of nanoparticle formation. In [19], for example, it was shown that the spectra of silver particles with a diameter from 21 to 2.2 nm embedded into the glass correspond to metal with an ordinary conduction band. In this work, we used a plasmonic model to determine the role of the average size of pores in the formation of the linear sizes of metal nanoparticles. For the sample under consideration, the size of pores is 4 nm, therefore the use of a plasmonic model seems to be adequate.

Currently, there are two main approaches to analyzing plasmonic properties of nanoparticles. The earlier method (which is widely used up to the present) is based on solving Maxwell's equations by analytical or numerical methods. One of the fundamental results in this case was obtained by Mie for the scattering of an electromagnetic wave on a spherical particle [20]. Somewhat later, an analogous solution was obtained for an ellipsoid by Gans [21]. Another approach (the  $\epsilon$ -method) is based on field expansion over the eigenfunctions with eigenvalues of the dielectric permittivity [22]. In some cases this method is convenient due to the possibility of obtaining a solution, which is due to the geometry of the system being universal with respect to the materials that the particles and the environment consist of.

In the case of particles whose dimensions are considerably lower than the wavelength, an external electromagnetic field is homogeneous. In this case, the only possible is the dipolar excitation. The polarizability of spherical particle is  $\alpha = \frac{\epsilon(\omega) - \epsilon_m}{\epsilon(\omega) + 2\epsilon_2} r^3$ , where  $r$  is

the spherical radius,  $\epsilon(\omega)$  and  $\epsilon$  are the dielectric permittivities of the metal and medium in which the particle is embedded. The extinction and scattering cross sections  $\sigma_a$  and  $\sigma_s$  of spherical particles have the form [23]

$$\sigma_a = 4\pi k \text{Im}\alpha,$$

$$\sigma_s = \frac{8\pi}{3} k^4 |\alpha|^2,$$

where  $k$  is the wave vector.

In a disordered grid of cylindrical pores of nanoporous Vycor, the formation of particles with random orientation elongated or flattened along the pores looks very probable. An approximation of spherical shape is useful for the simulation of such particles. In this case,

the polarizability is  $\alpha_{x,y} = \frac{\epsilon(\omega) - \epsilon_m}{3(\epsilon_m + L_1(\epsilon(\omega) - \epsilon_2))} \beta r^3$ ,

$\alpha_z = \frac{\varepsilon(\omega) - \varepsilon_m}{3(\varepsilon_m + L_0(\varepsilon(\omega) - \varepsilon_2))} \beta r^3$  where  $r$  is the circular cross-sectional radius of a spheroid,  $\beta$  is the aspect ratio, and the  $z$  axis is parallel to the direction of elongation or flattening of the spheroid. Depolarization coefficients are expressed through the aspect ratio of spheroid:  $L_0 = (e^2 - 1) \left( \frac{e}{2} \ln \left( \frac{e+1}{e-1} \right) - 1 \right)$ ,  $e = \frac{\beta}{\sqrt{\beta^2 - 1}}$  for an elongated, and  $L_0 = (e^2 + 1)(1 - e \operatorname{arccot} e)$ ,  $e = \frac{\beta}{\sqrt{1 - \beta^2}}$  for a flattened spheroid. Moreover,  $L_1 = \frac{1}{2}(1 - L_0)$  [21]. The absorption and scattering cross sections for an ensemble of spheroids with random orientation have the form [24]:

$$\sigma_a = 4\pi k \operatorname{Im} \left( \frac{2}{3} \alpha_{x,y} + \frac{1}{3} \alpha_z \right),$$

$$\sigma_s = \frac{8\pi}{3} k^4 \left( \frac{2}{3} |\alpha_{x,y}|^2 + \frac{1}{3} |\alpha_z|^2 \right).$$

It should be noted that in this model the size of spherical or spheroidal particles does not affect the width of resonance peaks, since it is in any case much smaller than the wavelength. Moreover, from the above expressions for the cross sections it follows that for the particles with a typical size of a few nanometers the absorption cross section (proportional to the particle volume) is significantly higher than the scattering cross section (proportional to the volume squared). Therefore, the observed extinction is almost entirely determined by the absorption.

Dependence of  $\varepsilon(\omega)$  of silver is well described by the model of free electrons with the contribution of the ionic lattice up to energies of  $\sim 4$  eV ( $\lambda \sim 300$  nm) when the interband transitions become significant:

$$\varepsilon(\omega) = \varepsilon_i - \frac{\omega_{\text{pl}}^2}{\omega^2 + i\omega\tau^{-1}}, \quad (1)$$

where  $\varepsilon_i \approx 3.7$  (for silver) is the phenomenological value describing the contribution of ions,  $\omega_{\text{pl}} \approx 13.8$  fs $^{-1}$  ( $\sim 9$  eV) is the plasma frequency,  $\tau \approx 36$  fs is the relaxation time of electrons [26], which corresponds to a free path length of  $\sim 50$  nm [27].

If the particle size is comparable with the free path length of electrons, an important role is played by scattering on the surface, which affects the imaginary part of  $\varepsilon(\omega)$ . This effect can be estimated with allowance for a decrease in the damping time in the model of free electrons [28]

$$\frac{1}{\tau} = \frac{1}{\tau_b} + \frac{A}{L_{\text{eff}}} V_F, \quad (2)$$

where  $\tau_b$  and  $\tau$  are the decay times of the bulk metal and metal nanoparticles,  $V_F$  (1.4 nm/fs for silver) is the Fermi velocity,  $A \sim 1$  is the phenomenological constant (its influence on the result is discussed in Section 3), which determines the scattering on the particle surface, and  $L_{\text{eff}}$  is the mean free path of electrons, which is of the order of the linear size of the particle. A review of some results that were obtained by different methods and estimated length  $L_{\text{eff}} = \frac{4V}{S}$  (where  $V$  and  $S$  are the volume and surface area of the particle) was given in [29]. This relationship is used in the further calculations.

Measured extinction spectra represent the dependence of the degree of exponent on the wavelength in the Bouguer–Lambert–Beer law

$$I = I_0 \exp(-\gamma z).$$

In the case of monodisperse particles, the coefficient  $\gamma = \gamma(\lambda)$  is determined by the extinction cross section of particles  $\sigma = \sigma_a + \sigma_s$  (if the processes of absorption and scattering are uncorrelated) and their concentration  $\gamma = \sigma N$ . In the case where there are particles with different shapes, each group of particles will make an additive contribution to extinction and the general expression for  $\gamma$  is obtained by integration. In modeling an ensemble of spheroidal particles, the distribution in the shape of particles can be represented as the distribution of aspect ratios  $\beta$ . This description shows a good agreement with electron-microscopy data and allows one to find the degree of elongation of a nanoparticle. Due to this, extinction spectroscopy is often used for rapid diagnostics of ensembles of elongated multi-dispersed particles [6–9].

### 3. RESULTS AND DISCUSSION

The absorption spectrum (Fig. 1, curve 1) was measured after the impregnation of the sample with the precursor solution in ethanol. The sample was then annealed for about 20 minutes at a temperature of 70°C until a pronounced yellow hue was observed. The absorption spectrum of the composite (Fig. 1, line 2) is markedly different from the spectrum measured before annealing. The difference of spectra represents the sharp peak at a wavelength of 400 nm (Fig. 1, curve 3), which clearly shows the presence of silver nanoparticles within the sample. As mentioned in the previous section, the scattering contribution to extinction is negligible in this case because of the smallness of nanoparticles. Therefore, the obtained results characterize the absorption. Closeness of the absorption peak profile to the Lorentz contour allows one to assume that the shape of particles differs slightly from spherical. Even at a small elongation degree of the particles [6–9] the spectrum acquires a two-peak structure caused by the presence of two modes for each

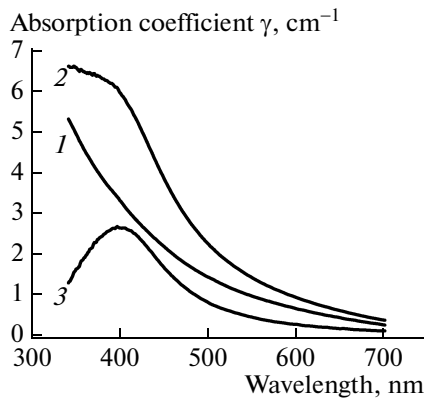


**Fig. 1.** Extinction spectra of a sample after the impregnation of precursor (1), and after annealing of the sample (2). The difference of these spectra (3) corresponds to the extinction spectrum of nanoparticles that formed after annealing.

nanoparticle (a longitudinal mode and a double-degenerated transverse mode).

Calculation of the spectra was performed using the model concepts described in Section 2. For a reference, the spectra were calculated without taking into account the scattering of electrons on the surface of nanoparticles ( $L_{\text{eff}} = \infty$  (3)), and the spectrum for a nanoparticle with radius  $r = 2$  nm, which is close to the mean radius of nanopores (Fig. 2). The spectral broadening in the first case is due solely to the imaginary part of the dielectric constant of silver. In the second case, the size effect dominates, which is clearly evident from spectral broadening. In this case, both of the calculated spectra are considerably narrower than the experimental spectrum, with a width of 130 nm. Let us discuss the factors that cause the wide absorption peak. First, a wide spectrum can be caused by a smaller particle size. The simulation results show agreement with the experiment in the case of spherical particles of radius 0.75 nm (Fig. 2). Second, spectral broadening may be caused by the deviation from the spherical shape of particles. For simulating aspherical spheroids, the model with a Gaussian distribution of the aspect ratio  $\beta$  with respect to the average value was used. The agreement with experiment is obtained for an ensemble of spherical particles with the maximum radius of circular cross-section of  $r = 1$  nm. The average value of the aspect ratio is  $\beta = 1$  and corresponds to a sphere, while the width (FWHM) is  $\Delta\beta = 0.7$ .

At larger sizes of spheroids ( $r > 1$  nm), the calculated absorption spectrum proves to be either narrower than the experimental one or it is significantly asymmetric. The reason that nanoparticles are formed in the pores with a diameter smaller than the average diameter of pores may be due to the fact that the most favorable conditions of growth exist in the narrowest parts of the porous grid. This assumption is confirmed

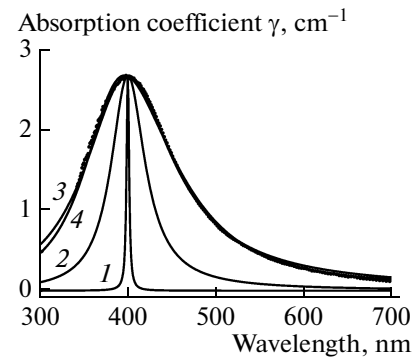


**Fig. 2.** Experimental (points) and calculated (lines) extinction spectra for silver particles: (1) without scattering from the surface; (2) for the spheres with a radius of 2 nm; (3) for the spheres with a radius of 0.75 nm in the case of spheroids with a radial cross-section of 1 nm and a Gaussian distribution with an average aspect ratio of 1 and the width of distribution (FWHM) of 0.7.

by the analysis of spectra at different concentrations of particles in the pores. The impact of concentration can be traced by comparing the results with those in [15, 16], where the samples were fabricated using the same technique but supercritical carbon dioxide was used as the solvent for impregnation. The obtained composites consist of identical components; thus, a comparative analysis of the spectra seems to be justified. Naturally, an increase in the concentration of nanoparticles in the sample leads to an increase in absorption (Fig. 3). However, it is accompanied by a marked shift in the spectrum towards longer wavelengths and still greater broadening of the absorption peak to  $\sim 200$  nm. This difference in the spectra cannot be explained by the variation in the sizes of nanoparticles in the limits of several nanometers, since particle growth to tens of nanometers inside the pores is impossible. Therefore, the observed shift, as well as the

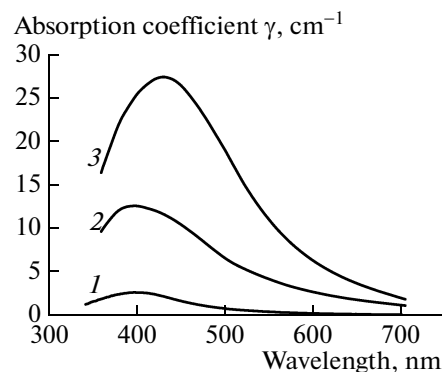


**Fig. 3.** Experimental extinction spectra of nanoparticles in nanoporous Vycor that was obtained in this work (1) and in [15] after annealing at a temperature of 90°C with durations of 15 (2) and 25 (3) minutes.

broadening, are associated with the formation of multiparticle clusters. Really, plasmon properties of the system of two or more neighboring particles differ considerably from the properties of each particle [17]. According to the calculation, the volume fraction of metal particles in the pores in the three cases examined by us is of order  $6 \times 10^{-8}$ ,  $4 \times 10^{-7}$ , and  $8 \times 10^{-7}$  (Figs. 3a, 3b, 3c, respectively). Each of these values is sufficiently small, but the difference between them is substantial. This may occur if nanoparticles fill the free volume of the sample non-uniformly, being concentrated in certain areas, probably in the places with the greatest narrowing. In this case, local concentration of particles may significantly exceed the aforementioned average values and closely located silver particles of a multiparticle cluster are formed in these areas.

It is worth noting that the position of an absorption peak maximum considerably depends on the dielectric permittivity  $\epsilon_m$  of the environment and on  $\epsilon_i$  in (1). We used the value  $\epsilon_i = 3.7$  in calculating profiles of the spectra and other parameters of silver were taken from [26]. A correspondence between the calculated and experimental absorption peaks was obtained at  $\epsilon_m = 2.45$ . In [30], another value,  $\epsilon_i = 4.45$ , of silver is given, which results in  $\epsilon_m = 2$ . In total, the magnitude of  $\epsilon_m$  in the present work weakly differs from the value  $\epsilon_m = 2.25$  [19] for a composite with a similar composition. In this case, the values of  $\epsilon_m$  and  $\epsilon_i$  considerably influence the peak position, and weakly affect the peak profile. Therefore, the accuracy of these values is not fundamental to the analysis that was carried out in this work.

In the calculation we used the value  $A = 1$ . This parameter is used to describe the influence of the size effect on the damping time reduction in the model of free electrons (see (2)). However, there are different values of  $A$  in various works; a typical range is  $0.1 < A < 1$  [17, 31–34]. If we assume that this value is less than unity, the profile of experimental spectrum corresponds to still smaller particles. The observed broadening of the absorption spectrum can also be due to the fact that nanoparticles formed in the pores are so small that a description within the model presented here excluding the effects of size quantization is incorrect. In general, the results of this work allow us to estimate the maximum value of the linear sizes for forming metal nanoparticles; however, estimation of the minimum size of these particles using this analysis is impossible.

## CONCLUSIONS

By performing the impregnation of nanoporous glass (with pores of a 4-nm radius) with a silver-containing alcohol solution of precursor and subsequent annealing at 70 °C, we obtained a transparent metal-dielectric composite. The extinction spectrum of the sample contains a sharp peak, which points to the for-

mation of silver nanoparticles. Analysis of the spectrum shows that the size of nanoparticles is significantly smaller than the average pore diameter and the shape is not very different from a spherical shape. The experimental spectrum corresponds well to spherical particles of 1.5 nm diameter or spheroidal particles with a diameter of less than 2 nm with a Gaussian distribution, a mean aspect ratio of 1 and a width (FWHM) of not more than 0.7. The behavior of extinction spectra by varying the concentration of nanoparticles also shows that they are formed in the narrowest areas of the porous grid. The local concentration of nanoparticles in the areas with conglomeration considerably exceeds the average value, which contributes to the cluster formation from closely spaced nanoparticles. Thus, the assumption that was made in several works that the restoration of silver atoms from a precursor leads to the formation of spherical nanoparticles in nanopores with a size that is equal to the average diameter of pores is not well justified.

## ACKNOWLEDGMENTS

This work was supported by the Russian Foundation for Basic Research (projects nos. 11-02001309-a, 13-02-12057ofi-m).

## REFERENCES

1. A. O. Rybaltovskii, S. S. Ilyukhin, N. V. Minaev, M. I. Samoilovich, M. Yu. Tsvetkov, and V. N. Bagratashvili, *Russ. J. General Chem.* **83**, 2212 (2013).
2. A. O. Rybaltovskii, V. N. Bagratashvili, S. S. Ilyukhin, D. A. Lemenovskii, N. V. Minaev, V. V. Firsov, and V. O. Yusupov, *Nanotechnology in Russia* **80**, 5353 (2013).
3. V. N. Bagratashvili, N. V. Minaev, A. O. Rybaltovskii, and V. I. Yusupov, *Laser Phys. Lett.* **8** (12), 853 (2011).
4. L. N. Zabukovec and V. Kaucic, *Acta Chim. Slov.* **53**, 117 (2006).
5. D. P. Broom and K. M. Thomas, *MRS Bulletin* **38** (5), 412 (2013).
6. S. Link, M. B. Mohamed, and M. A. El-Sayed, *J. Phys. Chem. B* **103**, 3073 (1999) with Corrections S. Link and M. A. El-Sayed, *Phys. Chem. B* **109** (20), 10531 (2005).
7. N. Xu, B. Bai, Q. Tan, and G. Jin, *Optics Express* **21**, 2987 (2013).
8. D. P. Sprunken, H. Omi, K. Furukawa, H. Nakashima, I. Sychugov, Y. Kobayashi, and K. Torimitsu, *J. Phys. Chem.* **111**, 14299 (2007).
9. S. Eustis and M. A. El-Sayed, *J. Appl. Phys.* **100**, 044324 (2006).
10. O. Pena, L. Rodriguez-Fernandez, V. Rodriguez-Iglesias, et al., *Appl. Opt.* **48** (3), 566 (2009).
11. V. P. Drachev, U. K. Chettiar, A. V. Kildishev, H. K. Yuan, W. Cai, and V. M. Shalae, *Opt. Express* **16** (2), 1186 (2008).

12. P.-E. Mota-Santiago, A. Crespo-Sosa, J.-L. Jiménez-Hernandez, H.-G. Silva-Pereyra, J.-A. Reyes-Esqueda, and A. Oliver, *Appl. Surf. Sci.* **259**, 574 (2012).
13. T. H. Elmer, Porous and reconstructed glasses, in *Ceramics and Glasses. Engineered Materials Handbook*, Ed. by S. J. Schneider, Jr., Vol. 4, 1991.
14. A. O. Rybaltovskii, A. A. Aksenov, V. I. Gerasimova, V. V. Zosimov, V. K. Popov, A. B. Solovyeva, P. S. Timashev, and B. N. Bagratashvili, *Supercritical Fluids Theory and Practice* **3**, 74 (2008).
15. A. O. Rybaltovskii, Yu. S. Zavorotnyi, N. V. Minaev, M. I. Samoilovich, P. S. Timashev, M. Yu. Tsvetkov, and B. N. Bagratashvili, *Russ. J. Phys. Chem. B* **3** (7), 1106 (2009).
16. A. O. Rybaltovskii, L. D. Bogomolova, V. A. Jachkin, V. V. Tarasova, N. V. Minaev, M. Yu. Tsvetkov, V. N. Bagratashvili, and M. I. Samoilovich, *Optical Mater.* **34** (1), 169 (2011).
17. V. V. Klimov, *Nanoplasmonics: Fundamentals and Applications* (Singapore, 2012).
18. A. Kawabata and R. Kubo, Electronic properties of fine metallic particles. II. Plasma resonance absorption, *J. Phys. Soc. Jpn.* **21**, 1765 (1966).
19. U. Kreibig, *J. Phys. F: Metal Phys.* **4**, 999 (1974).
20. G. Mie, *Ann. Phys. (Leipzig)* **25**, 377 (1908).
21. R. Gans, *Ann. Phys. (Leipzig)* **37**, 881 (1912).
22. N. N. Voitovich, B. Z. Katsenelenbaum, and A. N. Sivov, *Generalized Method of Eigen Oscillations in Diffraction Theory* (Nauka, Moscow, 1977) [in Russian].
23. L. D. Landau and E. M. Lifshitz, *Course of Theoretical Physics. Vol. 8: Electrodynamics of Continuous Media* (Pergamon, New York, 1984).
24. C. F. Bohren and D. R. Huffman, *Absorption and Scattering of Light by Small Particles* (Wiley, 1983).
25. P. B. Johnson and R. W. Christy, *Phys. Rev. B: Solid State* **6**, 4370 (1972).
26. C. von Sonnichsen, Plasmons in metal nanostructures. *Ph. D. Thesis*, (Munich, 2001).
27. U. Kreibig and M. Vollmer, *Optical Properties of Metal Clusters*, (Springer-Verlag, Berlin, 1995).
28. L. Genzel, T. P. Martin, and U. Kreibig, *Zt. Phys.* **21**, 339 (1975).
29. E. A. Coronado and G. Schatz, *J. Chem. Phys.* **119**, 3926 (2003).
30. P. Winsemius, Temperature dependence of the optical properties of Au and Ag *Ph. D. Thesis*, (University of Leiden, 1972).
31. C. Novo, D. Gomez, J. Perez-Juste, Z. Zhang, H. Petrova, M. Reismann, P. Mulvaney, and G. V. Hartland, *Phys. Chem. Chem. Phys.* **8**, 3540 (2006).
32. K.-P. Charle, L. Konig, S. Nepijko, et al., *Crystal Research and Technology* **33**, 1085 (1998).
33. B. N. J. Persson, *Surface Science* **281** (1, 2), 153 (1993).
34. O. A. Usov, A. I. Sidorov, A. V. Nashchekin, O. A. Podsvirov, N. V. Kurbatova, V. A. Tsekhomsky, and A. V. Vostokov, *Proc. of SPIE. Plasmonics: Metallic Nanostructures and Their Optical Properties VII.* **7394**, 73942J (2009). DOI: 10.1117/12.825988

*Translated by G. Dedkov*